

## An Empirical Formula for Assessing the Characteristic Strength of Unreinforced Laterite Stone Masonry

Hassane Seini Moussa <sup>1</sup>, Decroly Djoubissié Denouwé <sup>1</sup>, Abdou Lawane <sup>1\*</sup>,  
Anne Pantet <sup>2</sup>, Mamadou Diop <sup>1</sup>, Koami Wisdom Boko <sup>1</sup>

<sup>1</sup> *Laboratoire Eco-Matériaux et Habitats durables (LEMHaD), Institut international d'Ingénierie de l'Eau et de l'Environnement (2iE), Rue de la Science, 01 BP 594 Ouagadougou, Burkina Faso.*

<sup>2</sup> *Laboratoire Ondes et Milieux Complexes (LOMC), Université Le Havre Normandie, 25 Rue Philippe Lebon, 76600 Le Havre, France.*

Received 23 October 2023; Revised 12 March 2024; Accepted 18 March 2024; Published 01 April 2024

### Abstract

This study aims to determine the needed coefficients for evaluating the uniaxial compressive strength characteristic value for masonry structures made of Laterite Stone (LS) and cement mortar, resulting from experiments conducted in the laboratory evaluating the compressive strengths of the laterite stone and mortar separately in masonry. It proposes calculation coefficients for the completion of Eurocode 6 data that fit the behavior of laterite stone-based masonry. The laterite stone blocks are extracted from three quarries in southern Burkina Faso. The dimensions of the masonry samples tested are 800 mm × 800 mm × 135 mm (±5 mm) with a cement mortar joint of 20 mm (±5 mm) thick. The different failure modes of masonry were also explored. The tests carried out on the masonry showed that the failure is initiated by vertical cracks through the block-mortar interface at a quarter of the width of the walls, generally at 40 to 60% of their maximum strength. The statistical analysis made through a linear regression from the standard model of approximation of the characteristic strength of masonry in Eurocode 6 was used to set out parameters for the empirical relation. The proposed formula considers the intrinsic properties of the block and the mortar, the thickness of the mortar, the dimensions of the masonry block, and the geometry of the masonry itself to evaluate its compression strength. The adequacy between the model and the experimental values is evaluated through the coefficient of determination and the standard error of 0.94 and 0.041 MPa, respectively.

*Keywords:* Laterite Stone; Masonry; Uniaxial Compression; Empirical Formula.

## 1. Introduction

Stone masonry is one of the oldest construction methods that has gained renewed interest in its environment-friendly status and the social and environmental challenges of eco-housing. In Burkina Faso, Laterite Stone (LS) has been one of the materials used for masonry purposes for millennia because of its wide availability in many regions [1]. The term “laterite” is described as a reddish ferruginous, vesicular, unstratified, and porous material with yellow ochers [2, 3]. It is a relatively soft material extracted manually or mechanically with pickaxes or saws, depending on the quarry, the availability of the materials or modern technologies, and the hardness of the stone. Variations in characteristics regarding the location of quarries, the geological history, the depth of extraction, the direction of loading about anisotropy plans, and the mineral composition have been studied in the past, and some interesting conclusions have been highlighted. The properties of laterite stone vary significantly within the same quarry depending on the extraction layer and the moisture content [1, 4–6].

\* Corresponding author: [abdou.lawane@2ie-edu.org](mailto:abdou.lawane@2ie-edu.org)

<http://dx.doi.org/10.28991/CEJ-2024-010-04-07>



© 2024 by the authors. Licensee C.E.J, Tehran, Iran. This article is an open access article distributed under the terms and conditions of the Creative Commons Attribution (CC-BY) license (<http://creativecommons.org/licenses/by/4.0/>).

In developing countries such as Burkina Faso, construction with earthen materials should represent a suitable solution for the problem of sustainable housing for the population since it is cheap and so-called sustainable. The socio-economic impact of constructions based on earthen materials in the context of Burkina Faso has been studied by authors such as Zoungrana, and it confirms the eco-friendly status of raw earth construction materials [7–9]. Furthermore, earthen materials such as LS present very good comfort properties for Sahelian cities, villages, and hot environments due to their hygrothermal properties [10–13]. If LS has so many advantages, why is it not one of the most used materials for construction in tropical countries such as Burkina Faso? Indeed, some difficulties slow its expansion as a construction material. Firstly, in most constructions in Burkina Faso, where it is used, it is considered an infill wall material that does not bear main structural loads. Secondly, its structural behavior, as in structural masonry, is not well known, and the existing calculation methods do not fit the behavior observed experimentally for LS masonry. Thirdly, as mentioned previously, LS mechanical properties vary greatly within the same quarry and from one quarry to another. Some studies conducted in the recent past have shown that the available formulas for calculating masonry structures in compression do not accurately report the behavior of laterite stone masonry; furthermore, they overestimate the LS masonry load-bearing capacity [1, 14]. Its use needs to be standardized to upgrade Laterite stone at a status of construction material for confident structures. More information is needed concerning the complex structures that LS and mortar joints form. This study generally aims to contribute to standardizing laterite stone as a construction material. The specific objectives are set to be the characterization of laterite stone and mortar joints for masonry purposes, an experimental study of several low-size walls made of laterite stone and cement mortar joints, statistical analysis of the experimental and literature results, and setting out an empirical formula for assessing the behavior of laterite stone masonry under compressive loads. The scientific literature studies various types of masonry made from natural stones.

Kabore et al. [14], studying LS-based masonry walls from the DANO quarries, set a starting point for understanding the mechanical behavior of LS masonry under uniaxial compressive load. This study focused on the performance and limits of LS masonry by determining the range of compressive strength of this masonry calculated through existing formulas for other masonry materials and then comparing the empirical values to those determined experimentally. Indeed, the compressive strength of masonry is generally assessed by carrying out tests on prisms or walls in the laboratory. However, they are rarely performed due to the complexity of these experiments and their time and resource-consumption. Therefore, since masonry's strength depends on its elementary elements' characteristics (i.e., blocks and mortar), empirical formulas have been developed to establish links between the compressive strength of blocks and mortar and the load-bearing capacity of bulk masonry. Kaboré et al. [14], the authors have shown that the existing calculation codes, such as Eurocode 6 [15] and CNERIB [16], as well as the formulas proposed in the literature [17–19] for evaluating the uniaxial compressive strength characteristic value for masonry, do not accurately report the behavior of LS masonry. Table 1 presents some empirical formulas proposed in the literature to predict the compressive strength of different types of masonry. Most of these formulas are expressed as power functions and use the compressive strength of the block and the mortar as input parameters and their geometric characteristics. Some of these expressions are linear [20, 21] or polynomials [22] and consider only the strength of the block and the mortar. Most of these analytical models can thus be expressed in the following form:

**Table 1. Some analytical models for predicting the characteristic strength of masonry**

Type of masonry	Formulas
Unperforated Solid Brick [17]	$0.32 \times f_b^{0.53} \times f_m^{0.21}$
Clay Brick [23]	$0.63 \times f_b^{0.49} \times f_m^{0.32}$
Fly Ash Blocks [24]	$1.34 \times f_b^{0.1} \times f_m^{0.33}$
Clay Brick [25]	$0.1 \times f_b^{0.34} \times f_m^{1.93}$
Cambodian Blocks [26]	$0.24 \times f_b^{0.59} \times f_m^{0.32}$
Clay Blocks [24]	$0.69 \times f_b^{0.6} \times f_m^{0.35}$
Any Masonry with A Thick Joint [15]	$k \times f_b^{0.65} \times f_m^{0.25}$
Compressed Earth Brick [28]	$0.2 \times f_b^{1.26} \times f_m^{0.15}$
Unreinforced Solid Masonry [29]	$0.63 \times f_b^{0.49} \times f_m^{0.32}$
Laterite Block [30]	$0.482 \times f_b^{0.729} \times f_m^{0.365}$
Earth Brick Stabilized with Cement [31]	$0.25 \times f_b^{1.03} \times f_m^{0.28}$
Arch Bridge Masonry [20]	$\frac{1}{3} \times f_b + \frac{2}{3} \times f_m$
Clay Brick [21]	$0.53 \times f_b + 0.93 f_m - 10.32$
Clay Brick [22]	$0.327 f_b (1 - 0.003 f_b + 0.015 f_m)$

Many other authors have proposed similar formulas for various materials [32–38].

$$f_k = k \times f_b^\alpha \times f_m^\beta \tag{1}$$

where  $f_k$  is the characteristic compressive strength value of the masonry,  $f_b$  is the characteristic compressive strength value of the block.  $f_m$  is the characteristic compressive strength value of the mortar,  $\alpha$ ,  $\beta$  are corrective factors related respectively to the block and the mortar.  $k$  depends on the geometrical characteristics of the block and the mortar, as mentioned in [15]. The general remark about these previous studies is that the value of  $\alpha$  is greater than the value  $\beta$ . The strength of the masonry would, therefore, be more sensitive to a variation in the strength of the block than of the mortar. Only Basha & Kaushik [24] and Llorens et al. [25] found contradictory results. For the formula proposed by Chourasia et al. [30], the data used are based on scattered values from the literature regardless of the original experimental conditions and standard used. However, the experimental conditions and the standard used for evaluating the characteristic mechanical values of the masonry constituents impact the outputs deeply. So, it is important to consider the concomitant properties of the block and mortar used in the constitution of the masonry. Also, the lack of accuracy in this study regarding the calculation of the approximation error of the formula makes its general use biased.

The main objective of this study is to propose an empirical, analytical model to evaluate the characteristic uniaxial compressive strength of LS masonry. This model is based on experimental values of the block and mortars' compressive strength while exploring their failure modes under uniaxial compression.

## 2. Materials and Methods

### 2.1. Materials

Three blocks (Figure 1) from three quarries in Burkina Faso were used to build the sample walls. The raw blocks from the quarry are sawed to a size of 135 mm × 135 mm × 290 mm (±5 mm). The coordinates of the quarries are presented in Table 2. Two cement mortars, MO1 and MO2, were mixed from sand of two types: river sand and crushed granite sand from a quarry. The particle size distribution curves of the sands used are shown in Figure 1. The studied sands have relatively similar particle sizes. The proportions for a mixture of mortars are a ratio from 1:5 to 1:6 for cement/sand and 2:3 for the water/cement ratio in mass. The variation in cement content has intentionally been made to ensure that the characteristic values of compression strength will differ at 28 days of age since the compressive strength of the mortar is highly sensitive to the cement-sand ratio. The cement used is a Portland CEM II-42.5 N cement.

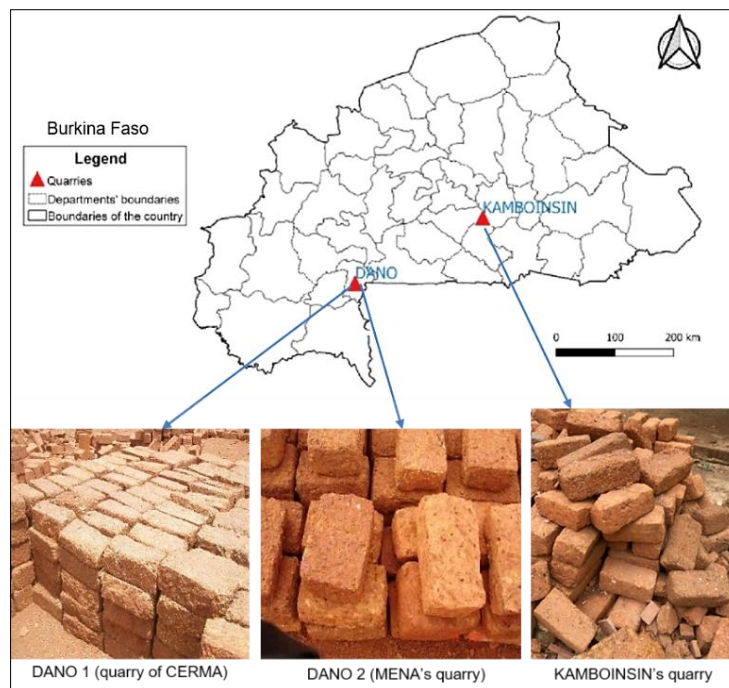
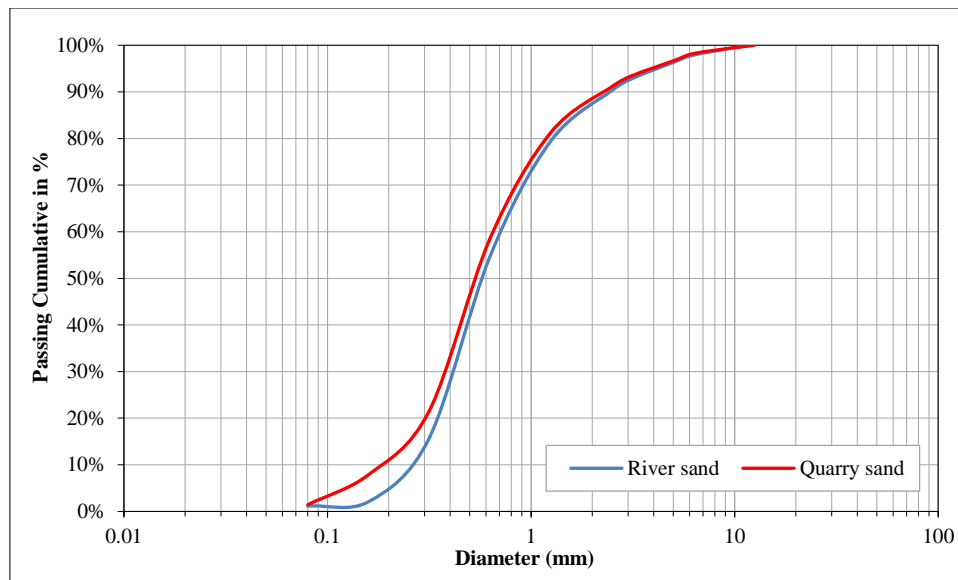


Figure 1. Blocks from the three quarries

Table 2. Location of the LS quarries

Quarry name	Latitude	Longitude	Altitude (m)
DANO 1 (CERMA Quarry)	11° 8'38.20"North	3° 3'59.50"West	322
DANO 2 (MENA Quarry)	11° 10'29.14"North	3° 2'32.78" West	278
KAMBOINSIN	12° 26' 48" North	1° 33' 45" West	301



**Figure 2. Particle size distribution curves of the sands used for mortar mix**

The dimensions of the sample walls tested are 800 mm × 800 mm × 135 mm ( $\pm 5$  mm) with a joint of 20 mm ( $\pm 5$  mm) thickness. The blocks' dimensions, the mortar's thickness, and the mix proportions have been chosen according to the construction practices commonly used in LS buildings in Burkina Faso. These values are also determined according to the European standard guidelines [39-42].

## 2.2. Experimental Methods

The compressive strengths of blocks, mortar, and masonry are determined according to European standards [43-45].

Figure 3(a) and (b) present the samples prepared for the compression test for the mortar and masonry units. For the compression test on masonry blocks, raw blocks from the quarries were cut into smaller parallelepipedal shape blocks of 70 mm x 70 mm x 70 mm ( $\pm 5$  mm) size (Figure 3b) with a mechanical saw. Then, the samples shaped for compressive strength tests in dry conditions are dried in an oven at  $70 \pm 2$  °C until reaching constant mass. Samples designed for compression strength tests in a saturated state are immersed in water for at least 48 hours until reaching constant mass. When the samples are ready for the tests, they are placed on a 300 kN load capacity hydraulic press cell and loaded at a loading rate of 0.05 mm/s until failure.



(a) Samples 40 × 40 × 160 (mm) for mortar compression test (b) Samples 70 × 70 × 70 (mm) for compression test on the block

**Figure 3. Samples for compression tests on blocks and mortar**

For the compression test on mortar samples, mortar is taken from the bulk mixture during the masonry sample wall construction and filled in three 40 mm × 40 mm × 160 mm ( $\pm 1$  mm) triplet mold (Figure 3a) and compacted on a shock table. The masonry mortar mix is carefully prepared to ensure accuracy and consistency in testing by combining the proportions of cement, sand, and water to create a homogeneous mixture. Firstly, the required quantity of cement is measured precisely using a scale. Next, the appropriate quantity of sand is added and thoroughly mixed with the cement until they form a uniform blend. Finally, water is gradually added to the mixture while continuously mixing until the desired consistency is achieved. The mold is filled with three layers of mortar, and each layer is compacted with 25 shocks by the shock table. For this study, regarding the low dispersion of measured strength among the collected samples onto the same quarry, the normalized strengths of the blocks are taken equal to the average value. However, in the general application of the formula, the characteristic values following the confidence interval will be the input data. A total of ten (10) walls were built by a professional mason for the experimentation. Six specimens were used for the

calibration of the formula and four for validating the model, in addition to results from the literature. Onto the same quarry, the mean strength for a load in a direction perpendicular to anisotropy plans of the stone (Figure 4a) or parallel to anisotropy plans (Figure 4b) is quite different. A wall is constructed for each quarry, whether with MO1 or MO2, and blocks are laid following a direction perpendicular or parallel to anisotropy plans. The device for the compression test on the wall is presented in Figure 5. The tests on the mortar and the wall are carried out after 28 days of maturation of the specimens and conserved at room temperature.

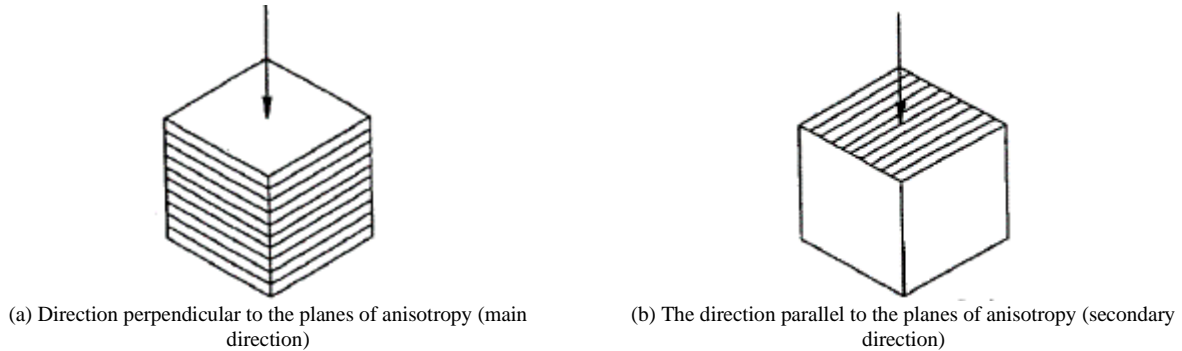


Figure 4. Direction of loading according to the anisotropy plan

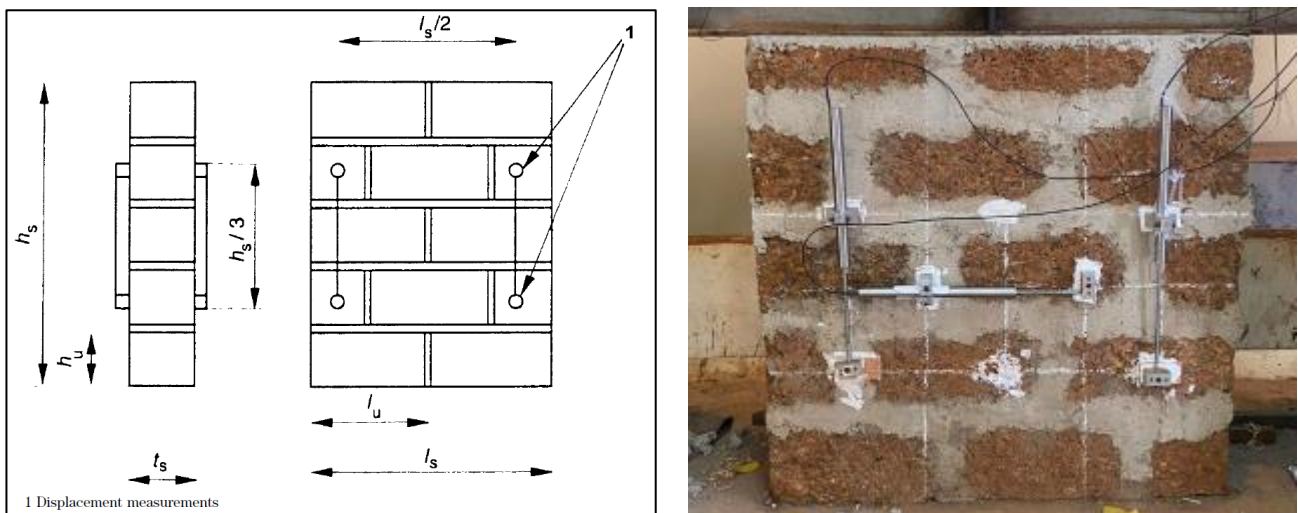


Figure 5. Device for compressive strength tests on walls

The specimens are equipped with four Linear Variable Differential Transformers (LVDT) displacement sensors placed in the vertical direction (2 on the front side and two on the back side) and an LVDT placed horizontally to measure the associated displacements (see Figure 5). The compressive load is applied gradually during the test by laps of 30% of the probable maximum load value from 0 to 30%, 30% to 60%, and then loaded until failure. The load is maintained constant for two minutes after each loading step. The compressive load is kept constant for two minutes to determine the deformations that have appeared and the creep degree. The maximum strength of the sample is obtained by dividing the load at the failure point by the loaded area of the sample. The characteristic strength equals the maximum strength divided by a safety factor 1.2 [45].

**2.3. Empirical Formula**

The empirical formula was determined based on the model defined in Equation 1. By composing this Equation by the natural logarithm function, it ends up with a linear equation with three variables:

$$\ln(f_k) = \ln(k) + \alpha \ln(f_b) + \beta \ln(f_m) \Rightarrow Z = \alpha X + \beta Y + K \tag{2}$$

where  $Z$  is  $\ln(f_k)$ ,  $f_k$  is the characteristic compressive strength of the masonry,  $X$  is  $\ln(f_b)$ ,  $f_b$  is the characteristic compressive strength of the block,  $Y$  is  $\ln(f_m)$ ,  $f_m$  is the characteristic compressive strength of the mortar,  $K$  is  $\ln(k)$ ,  $\alpha, \beta$  and  $k$  are the coefficients to be determined.

The least squares method was used to determine the scalars by minimizing the errors between the predicted values of the model and the experimental values.

The least squares method for similar models on  $n$  values is given by the expression in Equation 3.

$$S(X, Y, Z) = \sum_{i=1}^n e_i^2 = \sum_{i=1}^n (\alpha X_i + \beta Y_i + K - Z_i)^2 \quad (3)$$

The minimum of the function  $S$  is found when its partial derivatives regarding the parameters needed are equal to zero.

The system, therefore, summarizes as solving the following matrix Equation:

$$\begin{bmatrix} \sum_i X_i^2 & \sum_i X_i Y_i & \sum_i X_i \\ \sum_i X_i Y_i & \sum_i Y_i^2 & \sum_i Y_i \\ \sum_i X_i & \sum_i Y_i & n \end{bmatrix} \begin{bmatrix} \alpha \\ \beta \\ K \end{bmatrix} = \begin{bmatrix} \sum_i X_i Z_i \\ \sum_i Y_i Z_i \\ \sum_i Z_i \end{bmatrix} \quad (4)$$

The accuracy of the model was evaluated by using the coefficient of determination ( $R^2$ ), which is the percentage of variability explained by the model and the standard error of estimation ( $\sigma$ ) expressed in MPa and given by the following Equations:

$$R^2 = 1 - \frac{\sqrt{\sum (f_i - f_k)^2}}{\sqrt{\sum (f_i - f_{moy})^2}} \quad (5)$$

$$\sigma = \sqrt{\frac{\sum (f_i - f_k)^2}{n-3}} \quad (6)$$

where  $f_i$  is the strength of the masonry predicted by the model,  $f_k$  is the strength measured experimentally,  $f_{moy}$  the arithmetic mean value of the experimental strengths, and  $n$  is the number of data studied. A value of  $R^2$  close to 1 indicates a good fit of the model, and a value close to zero indicates a bad fit. At the same time, it is desirable that  $\sigma$  be as small as possible, implying that the data dispersion for the estimated value is minimal. The divisor  $n - 3$  is used in Equation 6 rather than  $n$  to get an unbiased estimation; the value “3” is chosen since three parameters are to be determined:  $K$ ,  $\alpha$ , and  $\beta$ .

### 3. Results and Discussion

#### 3.1. Failure Modes under Uniaxial Compression

Table 3 presents the compressive strength values of the LS blocks, mortar, and walls regarding the combinations. It is noticeable that there is no real impact on the type of sand used in the mix, whether it was the river's sand or quarry sand since there is no significant difference in their particle size distribution and for the same cement/sand ratio content, the compressive strength of the mortar are sensitively the same. Significant differences are noted when the cement/sand or water/cement ratio in mass varies.

**Table 3. Result of compression tests**

Quarry	Loading direction on the LS	Mortar	Block strength (MPa)	Mortar strength (MPa)	Characteristic strength of the wall (MPa)
DANO 1	Secondary	MO1	6.86	1.37	0.74
	Main	MO2	5.72	3.29	1.48
DANO 2	Secondary	MO2	5.50	1.37	0.62
	Main	MO1	2.18	3.03	0.88
KAMBOINSIN	Secondary	MO1	3.93	2.1	0.99
	Main	MO2	3.55	5.2	1.81

The failure modes observed during experiments are presented in Figure 6. The wall failure is initiated with vertical cracks parallel to the loading direction (Figure 6a). For walls assembled with blocks, they are laid in a direction parallel to the anisotropy planes of the blocks. In addition to longitudinal cracks, lateral cracks are crossing the thickness of the wall (Figure 6b). Most cracks are initiated in the upper quarter of the block's width (at the block-joint interface), between 40 and 60% of the breaking load on either side, and spread with ramifications up to the bottom of the wall. Similar observations have been made by Thamboo & Dhanasekar [28] on clay and compressed earth blocks and by Page [46] on terracotta blocks. Similar conclusions can be inferred from studies on some stone masonry structures [47].

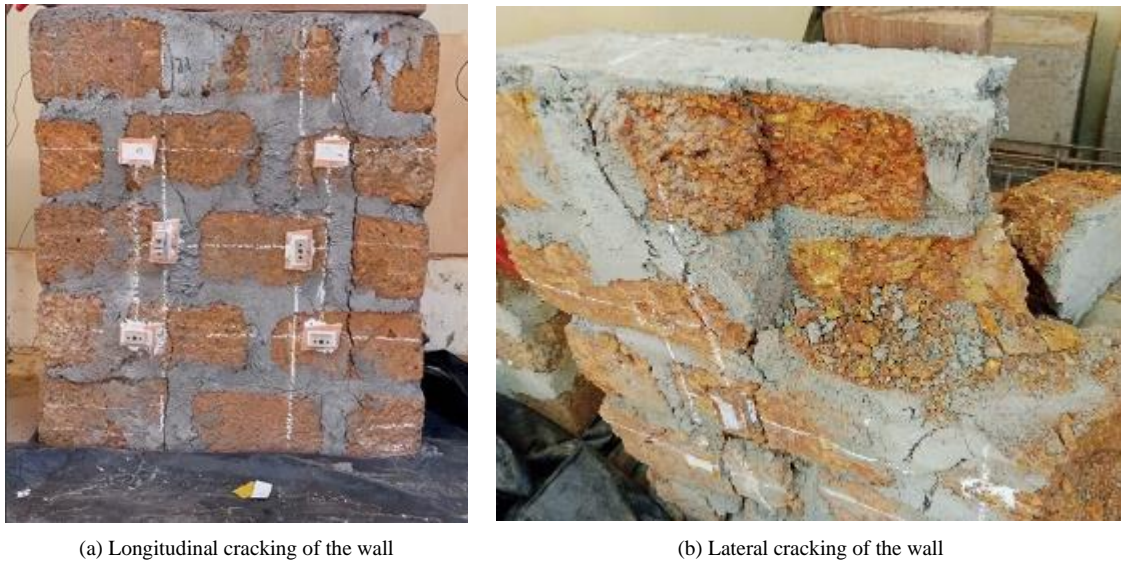


Figure 6. Failure mode of walls

Contrary to the works of Page [46], in most of the studied cases, the block presents a higher strength value than the mortar, which presents a higher strength value than the bulk masonry. Figure 7 presents the stress-strain curve of the tested walls. It should be noticed that the specimens constructed with blocks from DANO 1, which are the most rigid, present less deep axial deformations than those constructed with blocks from DANO 2, which are softer. In addition, the linear phase of the curve extends up to 100% of the failure strength for the walls of DANO 1 (brittle behavior) against 86% for the walls of DANO 2 (DANO 2 parallel direction taken as reference) with a slight ductility plateau after the peak (ductile behavior). These values are beyond the values observed by Kaushik et al. [23] (33%), Domède et al. [48] (40-50%), and Costigan et al. [49].

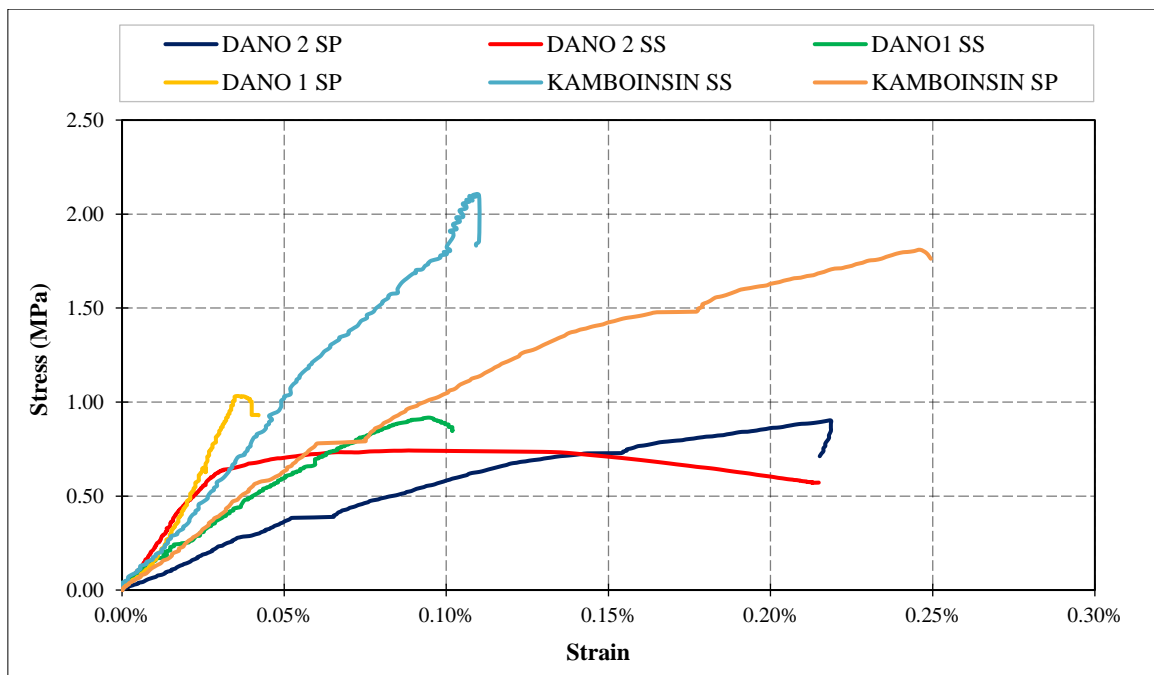


Figure 7. Stress-stain curves of the walls under uniaxial load

The notation "SP" and "SS" stand for "Main direction" and "Secondary direction," respectively, regarding the anisotropy plans presented in Figure 4.

### 3.2. Empirical Formula

The determined empirical formula (Equation 7) presents a greater sensitivity of the model to the strength of the mortar compared to the strength of the block with a coefficient of determination for the estimate  $R^2$  equal to 0.94 and an approximation error of estimation  $\sigma$  of  $4.13 \times 10^{-2}$  MPa. The values of  $\alpha$  and  $\beta$  proposed in the formula, obtained from the experimental campaign, show variations compared to the scientific literature. Contrary to the works of Pasala

Dayaratnam [29], who gives  $\alpha = \beta = 0,5$ , in this study,  $\alpha$  is sensitively half of the value of  $\beta$ ;  $\alpha \approx \frac{\beta}{2}$ . Even though the experimental tests conducted are limited, these variations show that the formulas proposed in the previous scientific literature do not correctly fit LS masonry behavior, including the results of Chourasia et al. [30], because of the biased input data used, as explained previously. It should also be noted that most of the studies on this subject are done on prism masonry. According to Thamboo & Dhanasekar [28], prisms overestimate the strength of masonry compared to walls.

$$f_k = 0.21(f_b)^{0.48}(f_m)^{0.94} \quad (7)$$

Furthermore, since primal failure signs appear at the interface between LS and vertical bed joint, the present solution seems more consistent than the formulas from prism masonry. The relationship established here was represented in 3 dimensions, with axis 1 for the compressive strength of the block, axis 2 for the compressive strength of the mortar, and axis 3 for the compressive strength of the masonry (Figure 8).

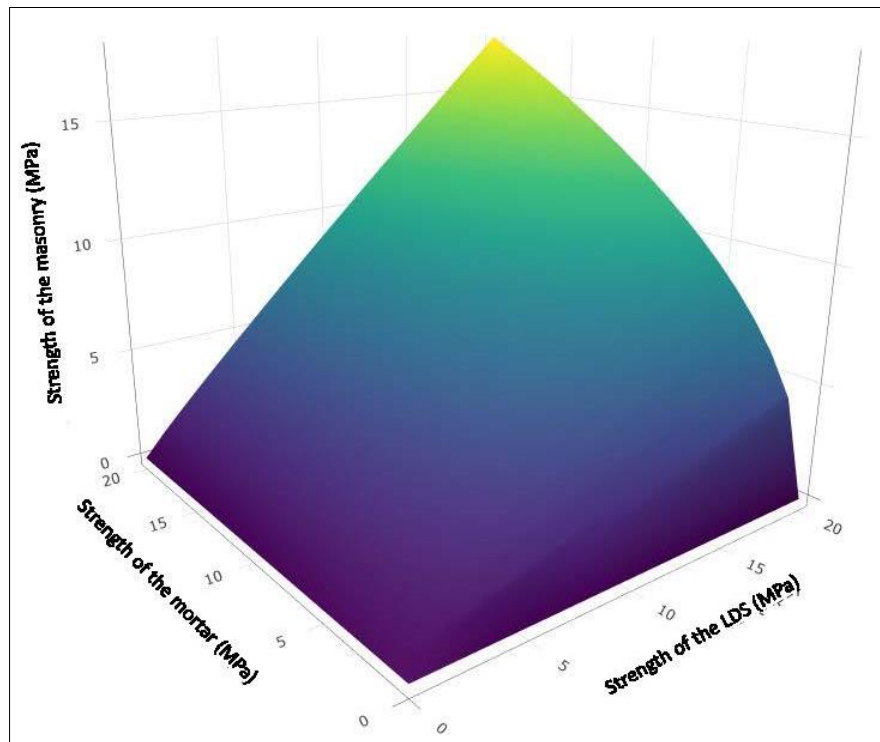


Figure 8. Graph showing the relationship between the strength of LS, mortar, and masonry

On the one hand, this figure shows a trend of logarithmic evolution of the masonry's compressive strength regarding the mortar's compressive strength in the plane formed by axes 2 and 3. On the other hand, Figure 8 shows a trend of linear evolution of the masonry's compressive strength regarding the block's compressive strength in the plane formed by axes 1 and 3. Regarding those profiles and based on the mathematical behaviors known of logarithm and linear functions and the fact that linear functions increase or decrease faster than logarithmic functions, it can be inferred that it is the strength of the laterite stone that primarily limits the resistance of the LS-based masonry since it reached its extremum values faster than the logarithm function of the mortar. Furthermore, the greater the mortar's compressive strength compared to the LS implies a better load-bearing capacity mobilization of the LS blocks and a more efficient structure. Thus, this induces greater resistance for the masonry. It is important to note that the European standard [15] avoids mortars over twice as strong as the masonry block. The opposite trend is observed when the masonry block is far stronger than the bed joint [50, 51].

Generally, the compressive strength of a masonry wall varies depending on different parameters. The compressive strength of the mortar used to bond the blocks plays a significant role in determining the overall compressive strength of the masonry wall. If the mortar is weaker than the blocks, it can become a weak link in the system, limiting the overall strength of the wall. The bond quality between the blocks and the mortar also affects the compressive strength of the masonry wall. Properly bonded blocks with good mortar joints can distribute loads more effectively and enhance the overall strength of the wall. The compressive strength of the individual blocks used in the masonry wall is crucial. Higher quality and stronger blocks will contribute to a stronger masonry wall overall. Weaker blocks may limit the overall strength of the wall, even if the mortar is strong. The construction techniques employed and the workmanship during the masonry wall assembly can impact its compressive strength. Proper installation methods, including correct mortar mixing and application, block placement, and curing practices, are essential for achieving optimal strength. The

design of the masonry wall, including factors such as wall height, thickness, reinforcement, and load-bearing requirements, can influence its compressive strength. A well-designed masonry wall, considering these factors, will typically have higher compressive strength. Overall, the compressive strength of a masonry wall about its constituent blocks and mortar is a complex interplay of various factors, and careful consideration of all these factors is necessary to ensure a structurally sound and strong masonry wall [52-54].

## 4. Conclusions

The main objective of this study was to propose an empirical, analytical model based on experimentations to calculate the characteristic compressive strength of unreinforced LS masonry having as inputs the compressive strength of blocks and mortar and exploring their different failure modes under uniaxial compression:

The analysis of the results allows the following conclusions to be drawn:

- The characteristic strength of LS-based masonry with thin joints (2 cm) and mortar of which the compressive strength does not exceed twice the strength of laterite stone block is quite accurate by the relation  $f_k = 0,21(f_b)^{0,48}(f_m)^{0,94}$  for 135 mm thick walls.
- The strength of the walls varies between 0.6 and 1.8 MPa, with a failure that generally begins at 40 to 60% of the maximum strength by the appearance of vertical cracks at a quarter of their width.
- The walls made with the blocks of DANO 1 have a brittle behavior, with a linear phase of the axial stress-strain curve reaching 100% of the breaking strength of the walls, contrary to the blocks of DANO 2, which are softer and have a ductile behavior. The blocks from KAMBOINSIN are in an interval between brittle and low ductile behavior.

However, to generalize the empirical formula to large-scale walls, it would be relevant to study the model's sensitivity to the variation in the size of the blocks and the mortar thickness. It should also be suitable for further studies to integrate as additional parameters various geometries of the wall that will impact the parameter "k" value.

## 5. Declarations

### 5.1. Author Contributions

Conceptualization, A.L. and A.P.; methodology, D.D.D. and M.D.; software, W.K.B.; validation, A.L., A.P., M.P., and D.D.D.; formal analysis, H.S.M.; investigation, H.S.M. and W.K.B.; resources, A.L.; writing—original draft preparation, H.S.M. and W.K.B.; writing—review and editing, A.L. and A.P.; supervision, A.L., D.D.D., and M.D.; project administration, A.L.; funding acquisition, A.L. All authors have read and agreed to the published version of the manuscript.

### 5.2. Data Availability Statement

The data presented in this study are available on request from the corresponding author.

### 5.3. Funding

The World Bank Group and Institute 2iE have funded the thesis of which this study is part.

### 5.4. Acknowledgements

The World Bank supported this work through its project "African Center of Excellence" (CEA-IMPACT) and College of Engineering (CoE).

### 5.5. Conflicts of Interest

The authors declare no conflict of interest.

## 6. References

- [1] Lawane Gana, A. (2014). Characterization of indurated lateritic materials for better use in housing in Africa. PhD Thesis, University of Le Havre, Le Havre, France. (In French).
- [2] Ndzié Mvindi, A. T., Onana, V. L., Ngo'o Ze, A., Ohandja, H. N., & Ekodeck, G. E. (2017). Influence of hydromorphic conditions in the variability of geotechnical parameters of gneiss-derived lateritic gravels in a savannah tropical humid area (Centre Cameroon), for road construction purposes. *Transportation Geotechnics*, 12, 70–84. doi:10.1016/j.trgeo.2017.08.003.
- [3] Oyelami, C. A., & Van Rooy, J. L. (2016). A review of the use of lateritic soils in the construction/development of sustainable housing in Africa: A geological perspective. *Journal of African Earth Sciences*, 119, 226–237. doi:10.1016/j.jafrearsci.2016.03.018.

- [4] Abhilash, H. N., McGregor, F., Millogo, Y., Fabbri, A., Séré, A. D., Aubert, J. E., & Morel, J. C. (2016). Physical, mechanical and hygrothermal properties of lateritic building stones (LBS) from Burkina Faso. *Construction and Building Materials*, 125, 731–741. doi:10.1016/j.conbuildmat.2016.08.082.
- [5] Lawane, A., Pantet, A., Vinai, R., & Thomassin, J. H. (2011). Geological and geomechanical study of Dano laterites (Burkina Faso) for use in housing. (In French).
- [6] Kasthurba, A. K., Santhanam, M., & Mathews, M. S. (2007). Investigation of laterite stones for building purpose from Malabar region, Kerala state, SW India - Part 1: Field studies and profile characterisation. *Construction and Building Materials*, 21(1), 73–82. doi:10.1016/j.conbuildmat.2005.07.006.
- [7] Vasanelli, E., Colangiuli, D., Calia, A., Sbartaï, Z. M., & Breyse, D. (2017). Combining non-invasive techniques for reliable prediction of soft stone strength in historic masonries. *Construction and Building Materials*, 146, 744–754. doi:10.1016/j.conbuildmat.2017.04.146.
- [8] Zoungrana, O., Bologo/Traoré, M., Messan, A., Nshimiyimana, P., & Pirotte, G. (2021). The Paradox around the Social Representations of Compressed Earth Block Building Material in Burkina Faso: The Material for the Poor or the Luxury Material? *Open Journal of Social Sciences*, 9(1), 50–65. doi:10.4236/jss.2021.91004.
- [9] Zoungrana, O., Bologo-Traore, M., Hema, C., Nshimiyimana, P., Pirotte, G., & Messan, A. (2020). Sustainable habitat in Burkina Faso: Social trajectories, logics and motivations for the use of compressed earth blocks for housing construction in ouagadougou. *WIT Transactions on the Built Environment*, 195, 165–172. doi:10.2495/ARC200131.
- [10] Ouedraogo, A. L. S.-N., Hema, C., N'guiro, S. M., Nshimiyimana, P., & Messan, A. (2024). Optimisation of Thermal Comfort of Building in a Hot and Dry Tropical Climate: A Comparative Approach between Compressed Earth/Concrete Block Envelopes. *Journal of Minerals and Materials Characterization and Engineering*, 12(1), 1–16. doi:10.4236/jmmce.2024.121001.
- [11] Nshimiyimana, P., Hema, C., Zoungrana, O., Courard, L., & Messan, A. (2022). Contribution to improving the quality of raw earth habitat in Burkina Faso. *NoMaD 2022*, 16-17 November, 2022, Montpellier, French. (In French).
- [12] Moussa, H. S., Nshimiyimana, P., Hema, C., Zoungrana, O., Messan, A., & Courard, L. (2019). Comparative Study of Thermal Comfort Induced from Masonry Made of Stabilized Compressed Earth Block vs Conventional Cementitious Material. *Journal of Minerals and Materials Characterization and Engineering*, 7(6), 385–403. doi:10.4236/jmmce.2019.76026.
- [13] Hema, C., Ouédraogo, A. L. S. N., Bationo, G. B., Kabore, M., Nshimiyimana, P., & Messan, A. (2024). A field study on thermal acceptability and energy consumption of mixed-mode offices building located in the hot-dry climate of Burkina Faso. *Science and Technology for the Built Environment*, 30(2), 184–193. doi:10.1080/23744731.2023.2291007.
- [14] Kaboré, M., Lawane, A., Sawadogo, C., Lo, M., Messan, A., & Pantet, A. (2019). Études expérimentales du comportement mécanique sous charges verticales des maçonneries en Blocs de Latérite Taillée (BLT). *Afrique SCIENCE*, 15(1), 201–213.
- [15] NF EN 1996-1-1+A1. (2013). Eurocode 6 - Design of masonry structures - Part 1-1: general rules for reinforced and unreinforced masonry structures. AFNOR Editions, Saint-Denis, France. (In French).
- [16] Alili, S. (2013). Technical guide for an operation to rehabilitate the village architectural heritage of Kabylie. Ph.D. Thesis, University of Tizi Ouzou, Tizi Ouzou, Algeria. (In French).
- [17] Hendry, A. W., & Malek, M. H. (1986). Characteristic Compressive Strength of Brickwork Walls from Collected Test Results. *International Masonry Institute*, 7, 15–24.
- [18] Lourenço, P. B., & Pina-Henriques, J. (2006). Validation of analytical and continuum numerical methods for estimating the compressive strength of masonry. *Computers and Structures*, 84(29–30), 1977–1989. doi:10.1016/j.compstruc.2006.08.009.
- [19] Mann, W. (1982). Statistical evaluation of tests on masonry by potential functions. Sixth international brick masonry conference, 16-19 May, 1982, Rome, Italy.
- [20] Engesser, F. (1907). Over long-span arched bridges. *Zeitschrift für Architekturs und Ingenieurwesen*, 53, 403-440. (In German).
- [21] Garzón-Roca, J., Marco, C. O., & Adam, J. M. (2013). Compressive strength of masonry made of clay bricks and cement mortar: Estimation based on Neural Networks and Fuzzy Logic. *Engineering Structures*, 48, 21–27. doi:10.1016/j.engstruct.2012.09.029.
- [22] Dymiotis, C., & Gutleiderer, B. M. (2002). Allowing for uncertainties in the modelling of masonry compressive strength. *Construction and Building Materials*, 16(8), 443–452. doi:10.1016/S0950-0618(02)00108-3.
- [23] Kaushik, H. B., Rai, D. C., & Jain, S. K. (2007). Stress-Strain Characteristics of Clay Brick Masonry under Uniaxial Compression. *Journal of Materials in Civil Engineering*, 19(9), 728–739. doi:10.1061/(asce)0899-1561(2007)19:9(728).
- [24] Basha, S. H., & Kaushik, H. B. (2015). Evaluation of Nonlinear Material Properties of Fly Ash Brick Masonry under Compression and Shear. *Journal of Materials in Civil Engineering*, 27(8), 4014227. doi:10.1061/(asce)mt.1943-5533.0001188.
- [25] Llorens, J., Llorens, M., Chamorro, M. A., & Soler, J. (2020). Experimental Behavior of Brick Masonry under Uniaxial Compression on Parallel-to-Face Brick. Single-Leaf Case Study. *International Journal of Architectural Heritage*, 14(1), 23–37. doi:10.1080/15583058.2018.1503361.

- [26] Kandymov, N., Mohd Hashim, N. F., Ismail, S., & Durdyev, S. (2022). Derivation of Empirical Relationships to Predict Cambodian Masonry Strength. *Materials*, 15(14), 5030. doi:10.3390/ma15145030.
- [27] Kumavat, H. R. (2016). An Experimental Investigation of Mechanical Properties in Clay Brick Masonry by Partial Replacement of Fine Aggregate with Clay Brick Waste. *Journal of The Institution of Engineers (India): Series A*, 97(3), 199–204. doi:10.1007/s40030-016-0178-7.
- [28] Thamboo, J. A., & Dhanasekar, M. (2019). Correlation between the performance of solid masonry prisms and wallettes under compression. *Journal of Building Engineering*, 22, 429–438. doi:10.1016/j.jobe.2019.01.007.
- [29] Dayaratnam, P. (1987). *Brick and reinforced brick structures*. South Asia Books, Delhi, India.
- [30] Chourasia, A., Singhal, S., & Chourasia, A. (2023). Numerical simulation of laterite confined masonry building subjected to quasi-static monotonic lateral loading. *Journal of Structural Integrity and Maintenance*, 8(1), 1–11. doi:10.1080/24705314.2022.2142895.
- [31] Sajanthan, K., Balagasan, B., & Sathiparan, N. (2019). Prediction of compressive strength of stabilized earth block masonry. *Advances in Civil Engineering*, 2019. doi:10.1155/2019/2072430.
- [32] Caldeira, F. E., Nalon, G. H., Oliveira, D. S. de, Pedroti, L. G., Ribeiro, J. C. L., Ferreira, F. A., & Carvalho, J. M. F. de. (2020). Influence of joint thickness and strength of mortars on the compressive behavior of prisms made of normal and high-strength concrete blocks. *Construction and Building Materials*, 234. doi:10.1016/j.conbuildmat.2019.117419.
- [33] Lawrence, S. J., & Page, A. W. (2008). *New Australian standards for masonry in small structures*. Proc. 14 IBMAC, Sydney, Australia.
- [34] Mojsilović, N., & Stewart, M. G. (2015). Probability and structural reliability assessment of mortar joint thickness in load-bearing masonry walls. *Structural Safety*, 52, 209–218. doi:10.1016/j.strusafe.2014.02.005.
- [35] Sarhat, S. R., & Sherwood, E. G. (2014). The prediction of compressive strength of ungrouted hollow concrete block masonry. *Construction and Building Materials*, 58, 111–121. doi:10.1016/j.conbuildmat.2014.01.025.
- [36] Thaickavil, N. N., & Thomas, J. (2018). Behaviour and strength assessment of masonry prisms. *Case Studies in Construction Materials*, 8, 23–38. doi:10.1016/j.cscm.2017.12.007.
- [37] Fortes, E. S., Parsekian, G. A., & Fonseca, F. S. (2015). Relationship between the Compressive Strength of Concrete Masonry and the Compressive Strength of Concrete Masonry Units. *Journal of Materials in Civil Engineering*, 27(9), 4014238. doi:10.1061/(asce)mt.1943-5533.0001204.
- [38] Rizaee, S., Hagel, M. D., Kaheh, P., & Shrive, N. (2016). *Comparison of compressive strength of concrete block masonry prisms and solid concrete prisms*. Brick and Block Masonry, CRC Press, Boca Raton, United States. doi:10.1201/b21889-228.
- [39] NF EN 771-6 + A1. (2015). *Specifications for masonry units - Part 6: natural stone masonry units*. AFNOR Editions, Saint-Denis, France. (In French).
- [40] NF EN 13373. (2020). *Test methods for natural stones - Determination of dimensions and other geometric characteristics*. AFNOR Editions, Saint-Denis, France. (In French).
- [41] NF EN 998-2. (2016). *Definitions and specifications of mortars for masonry - Part 2: mortars for mounting masonry units*. AFNOR Editions, Saint-Denis, France. (In French).
- [42] NF EN 772-16. (2011). *Methods of testing masonry elements - Part 16: determination of dimensions*. AFNOR Editions, Saint-Denis, France. (In French).
- [43] NF EN 772-1 + A1. (2015). *Methods of testing masonry units - Part 1: determination of compressive strength*. AFNOR Editions, Saint-Denis, France. (In French).
- [44] NF EN 1015-11. (2019). *Methods of testing mortars for masonry - Part 11: determination of flexural and compressive strength of hardened mortar*. AFNOR Editions, Saint-Denis, France. (In French).
- [45] NF EN 1052-1. (1999). *Masonry testing methods - Part 1: determination of compressive strength*. AFNOR Editions, Saint-Denis, France. (In French).
- [46] PAGE, A. (1981). The Biaxial Compressive Strength of Brick Masonry. *Proceedings of the Institution of Civil Engineers*, 71(3), 893–906. doi:10.1680/iicep.1981.1825.
- [47] Wang, Z., Li, L., Zhou, J., Chen, R., Leng, J., Zhang, H., & Yang, J. (2024). Experimental investigation and calculation method of the interfacial bonding performance of stone masonry reinforced with UHPC. *Journal of Building Engineering*, 85, 108435. doi:10.1016/j.jobe.2024.108435.
- [48] Domède, N., Pons, G., Sellier, A., & Fritih, Y. (2009). Mechanical behaviour of ancient masonry. *Materials and Structures/Materiaux et Constructions*, 42(1), 123–133. doi:10.1617/s11527-008-9372-z.

- [49] Costigan, A., Pavía, S., & Kinnane, O. (2015). An experimental evaluation of prediction models for the mechanical behavior of unreinforced, lime-mortar masonry under compression. *Journal of Building Engineering*, 4, 283–294. doi:10.1016/j.jobe.2015.10.001.
- [50] Zahra, T., Thamboo, J., & Asad, M. (2021). Compressive strength and deformation characteristics of concrete block masonry made with different mortars, blocks and mortar beddings types. *Journal of Building Engineering*, 38. doi:10.1016/j.jobe.2021.102213.
- [51] Álvarez-Pérez, J., Chávez-Gómez, J. H., Terán-Torres, B. T., Mesa-Lavista, M., & Balandrano-Vázquez, R. (2020). Multifactorial behavior of the elastic modulus and compressive strength in masonry prisms of hollow concrete blocks. *Construction and Building Materials*, 241. doi:10.1016/j.conbuildmat.2020.118002.
- [52] Abu-Bakr, M., Mahmood, H. F., Mohammed, A. A., & Ahmed, S. A. (2024). Evaluation of mechanical properties and shear-bond strength of mortar containing natural extract admixture. *Construction and Building Materials*, 418, 135377. doi:10.1016/j.conbuildmat.2024.135377.
- [53] Zhang, P., Fan, S., Liu, Y., Su, C., Hu, J., & Sheikh, S. A. (2024). Axial compressive performance of masonry columns strengthened with ECC jacket and FRP strips. *Engineering Structures*, 304, 117661. doi:10.1016/j.engstruct.2024.117661.
- [54] Corradi, M., Borri, A., & Vignoli, A. (2003). Experimental study on the determination of strength of masonry walls. *Construction and Building Materials*, 17(5), 325–337. doi:10.1016/S0950-0618(03)00007-2.